Joint Special Interest Group meeting between euspen and ASPE
Advancing Precision in Additive Manufacturing
KU Leuven, Belgium, September 2023
www.euspen.eu

Evaluating the shift in laser alignment during multi-laser powder bed fusion

Samuel Searle[1,2], Michele Vanini [1,2,3], Lars Vanmunster [1,2], Sven Cornelissen[4], Bey Vrancken [1,2]

[1] *Department of Mechanical Engineering, KU Leuven, Celestijnenlaan 300, 3001 Leuven, Belgium*
[2] *Flanders Make@KU Leuven*
[3] *Department of Materials Engineering, KU Leuven, Kasteelpark Arenberg 44, 3001 Leuven, Belgium* [4] *Materialise NV, Technologielaan 15, 3001 Leuven, Belgium*

samuel.searle@kuleuven.be

Abstract

Whilst enabling higher production rates, Multi laser powder bed fusion (MLPBF) machines are not without drawbacks. The increased complexity of operating multi laser printers is a poorly understood problem. In this study, a test print is proposed to be able to track shifts in the positional alignment between lasers during printing. After a total print height of 40mm containing 43790 mm² of layer area, the temperature on the outside of the scan box increased by 6°C. At the top of the print an average offset of 68 µm was observed between the two scan fields. This offset happened predominantly towards the bottom right of the baseplate. Consequently, the observed positional shift between the lasers raises concerns regarding the potential lack of fusion in neighbouring regions between hatches scanned with different lasers. Further investigation is required to understand the source and direction of this offset. Additionally, measurements of the relative position of the scan head will be correlated with the observed offse t to determine if heat accumulation and subsequent stretching of the scan box could be contributing factors.
In conclusion, the test print and analysis methodology presented in this study provide insights into the positional alignment shifts in MLPBF machines. The observed offset of 68 µm after 40 mm of printing highlights the potential for significant hatch separation, which may compromise part integrity. This research serves as an important step towards understanding and addressing the challenges associated with operating multi-laser printers, ultimately enabling improved printing accuracy and reliability.

Multi Laser Powder Bed Fusion, Scan field alignment, Optical metrology, Thermal lensing

1. Introduction

Multi-Laser powder bed fusion (MLPBF) is an advancement that has unlocked the potential of LPBF for serial part production due to its increased productivity. It has also created novel avenues of research in melt-pool shaping and in situ heat treatment. However, the addition of optical paths in MLPBF machines proportionally increases the complexity of setups, their maintenance and usage. With each scanner requiring individual calibration in terms of position, laser power and focus; before being synchronized and aligned with one another. This final step ensures that all scanners operate on the same coordinate system, especially important when multiple lasers operate on the same part. Inaccuracies in this final setup creates geometrical deviations as well as the possibility of lack of fusion in the neighboring region between two hatches scanned with different lasers.

A test print is proposed and demonstrated, to be able to track ex-situ the shift in laser coordinate systems.

2. Background

In single laser systems, beam focus is known to shift during the production process due to the thermal influence of the laser on the elements in the optical path. Thermal lensing affects the beam's size and melting power. The shift in beam size comes from bulging of transmissive optical elements due to thermal stress from the absorption of the laser light. Goossens et al. measured a response time of 38 seconds before the elements in the optical path reached their steady state after which a recoat time of 8 seconds was sufficient to retrieve the cold state of beam size. To correct these changes in beam size focus compensation was demonstrated as a viable solution [1].

However, an additional concern arises from heat dissipated from the optical elements as a fraction of the light they transmit, gets absorbed. This heat is diffused to the scan box. Which, alongside thermal conduction through the build chamber and back reflected light to the scan box can cause a slow increase in the temperature of metal on to which scan heads are mounted. This can potentially change the relative position of elements in the optical path.

In single laser machines, this phenomenon would cause slight shifts between the relative position of layers, leading to a minor loss in geometrical accuracy throughout the whole part. Conversely, in dual laser machines, there is the potential for the lasers to drift apart in the same layer, which can create the possibility of lack of fusion in the neighboring region between two hatches scanned with different lasers. Furthermore, with the development of novel multi-laser scan strategies that enable in-situ heat treatment, lasers now operate in close proximity to each other. Consequently, it becomes crucial to assess the shift between lasers to ensure accurate and consistent processing.

3. Methodology

This section describes the design and measurement procedure of a test print capable of highlighting deviations in scan field alignment during extended printing. The assessment will be conducted on a dual laser Print Genius 150 (Prima Additive, Torino, Italy) in 316L stainless steel. The printer is equipped with two scan fields capable of covering the entire print volume. They are positioned 20 mm to the left and 20 mm to the right of the base plate centre, respectively..

3.1 Test print design

The job is designed to allow the lasers to create alignment marks at increasing levels of the print. To differentiate transient effects during printing from possible initial misalignment of the lasers, it is necessary for these marks to be positioned in the same location on the base plate. The marks are scanned on top of small cylinders (⌀10 mm x 2.5 mm), referred to hereafter as "pucks." Pucks are separated vertically by 2.5 mm. Support structures are used between pucks, ensuring they do not interfere with the calibration marks. Ten pucks are arranged in a pillar with a total height of 50 mm.

An important consideration is the printed area, which is adjusted to be longer than the recoating time of 20 s. To increase the printed area, twenty-four pillars are printed. Twelve are positioned radially 65 mm from the centre of the base plate. An additional five are positioned radially 20 mm around the centre of each scan field, and one is placed at the centre of each scan field. Two rectangular prisms with a 20 mm x 20 mm base are also printed in conjunction with the pillars to ensure that the print area is not reduced significantly during the support layers of the pillars. The load balance was set so that scan field 0 (right of baseplate) printed more layers. This was done to extenuate any alignment offset due to a load imbalance. The pillars are printed using both lasers simultaneously, this ensures that the transient effects are minimised, as discussed in section 2. The positioning is visible in Fig. 1.a.

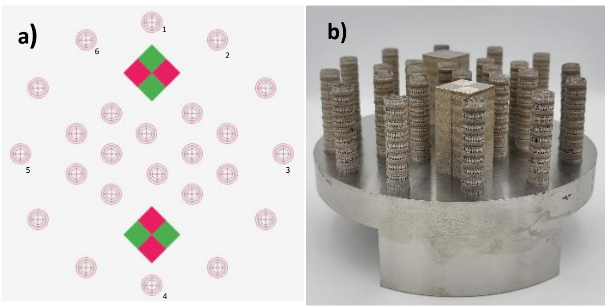

Figure 1. a) First layer of the print, as viewed in Materialise Inspector. Magenta corresponds to scan field zero and green corresponds to scan field one. **1. b)** Finished Print after powder removal.

3.2 Alignment mark

The alignment mark consists of two concentric rings: 7 mm and 8 mm in diameter, with two right angle lines intersecting at the centre Fig. 2. a. Each laser prints one ring and one set of lines. This enables the calculation of the laser offset from the distance between the circle centre or the distance between the two intersections. The lines are used to measure changes in the angle between the laser and align the images taken with the microscope. A custom script was created to add the marks to the .job file as a post-slicing step. The calibration marks are printed with a speed of 800 mm/s, a power of 280 W, and a beam diameter of 70 µm. They are printed on the layer above the final layer of each puck with a 30 µm layer height.

3.2 Analysis

3.2.1 Microscopy

Five pillars from the outer ring were randomly selected for this initial round of analysis. Their position is indicated in Fig. 1.a. The outer ring was selected because any rotational calibration shift would be more apparent in this region, as it's further away from the centre of rotation. Additionally, a sixth pillar from the ring was also analysed. Different surface treatments were trialled to increase the contrast between the underlying hatches and the rings of the alignment mark Fig. 2. b. Dying the top surface with a black permanent marker, then using a pencil eraser to expose the tracks of the alignment mark was found to provide the best contrast Fig. 2. c.

The pucks of the pillar were measured as described before but after the images were captured, the dye was wiped clean and reapplied, for another set of images to be taken. This process was repeated 11 times, to assess the standard error of the measurement. The pucks imaged with a Keyence VHX 6000 at 30x magnification. The whole puck was taken in one shot without stitching. Coaxial lighting was chosen and adjusted so that the rings of the marks were overexposed. Ring lighting was also tried; however, the shadow cast towards the centre created uncertainty about the width of the track.

3.2.2 Post Processing

Images were post processed using Fiji [2]. They were cropped and centred, but not rotated to avoid the introduction of interpolation artifacts.

Firstly, Colour thresholding was used to remove the blue glare in the centre of the images, which was caused by the coaxial lighting. The images were then thresholded, to keep only the overexposed areas of the alignment tracks shown in Fig. 2. d. Particle analysis was then used to mask out, small unconnected areas. Larger areas of pixel which remained connected to the ring were removed manually Fig 2. e. Finally, the images were sectioned, such that, the two rings, and the four lines composing the cross were saved separately as binary images, conserving their position in images of the same size as the source Fig. 2. f.

Each image was then processed using Python scripts. The white pixels of the images were converted to coordinates, and fitting algorithms were used to find the equation of the rings (represented by ellipses), the centre coordinates (x, y), semi-major and semi-minor axes of the lines. The lines were fitted using SciPy's linear regression function [3]. The points of the vertical lines, were first transposed so to have a finite slope. The slope and y-intercept were then converted back to the pre-transposed values. Least squares ellipse fitting was chosen over circle fitting for the rings, so that any error between the tilt of the puck and the optical plane would not result in a shift in the measurement of the centre position of the ring [4].

The Euclidean distance between the ring centres of each puck was calculated. These values were normalized with respect to the offset measured on the first puck of each pillar. The slope and y-intercept of the fitted line were used to calculate the angle of each puck when imaged. This was further used to calculate the x and y offsets of the ring centres in base plate coordinates.

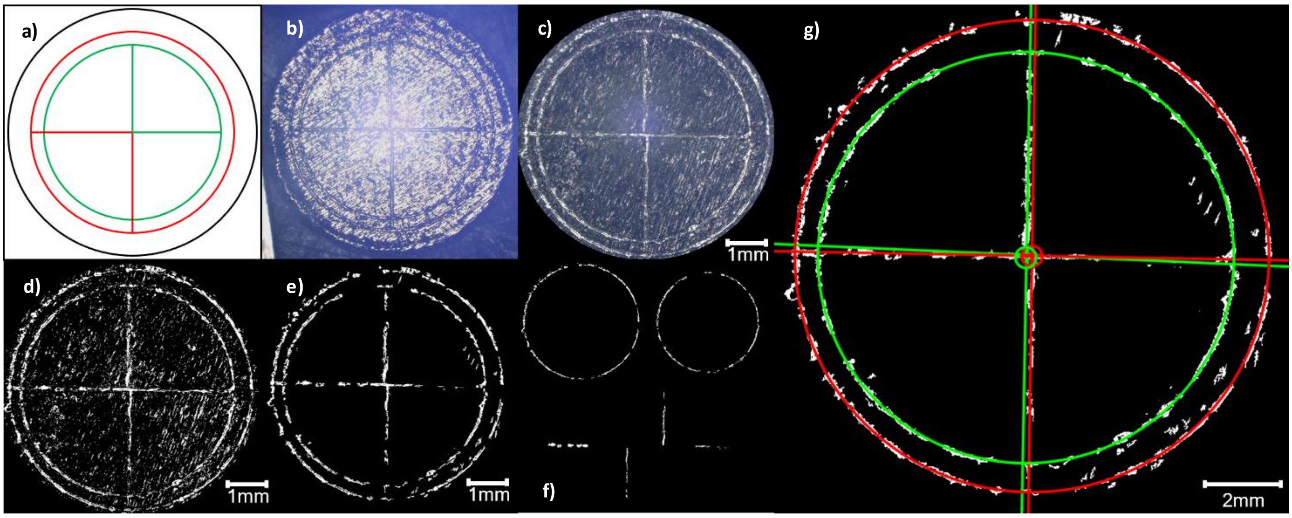

Figure 2. a) Scan vectors composing the alignment mark, with scan field 0 in red and scan field 1 in green **2. b)** Optical microscope image of the as printed puck (30x) **2. c)** Optical microscope image of the printed puck with contrast increasing surface treatment. **2. d)** Binary image of the puck after thresholding to enhance mark contrast. **2. e)** Alignment marks after particle removal. **2. f)** Separated alignment mark elements before curve fitting. **2. g)** Binary image from [2. e], with the fitted curves calculated from [2. f].

4. Results and Analysis

During the print, a previously unknown issue with the laser control board of the printer caused a printer failure during the night. While it was possible to restart the print, the thermal build-up was lost. Despite this setback the pillars reached 8 pucks in height, generating sufficient data for the analysis this is visible in Fig. 1.a. Furthermore, the support structure of the first puck, attached to the build interfered with the alignment marks which were printed on the first layer. These were also excluded from the study limiting the experiment from the first puck at a height of 5 mm puck to a final height of 45 mm puck.

Analysis of the .job file reveals that the total print area at puck number 8 after a print height of 40 mm is 43790 mm^2 equivalent to 9.24 kJ of laser energy, being directed through the optical path of the laser. A noticeable difference in scan box temperature was measured by a k type thermocouple attached to outside wall of the scan box. The readings of this show an increase from 30 °C to 36 °C visible in Fig. 3. This temperature increase would be even more pronounced if it was taken from inside, closer to the optical path.

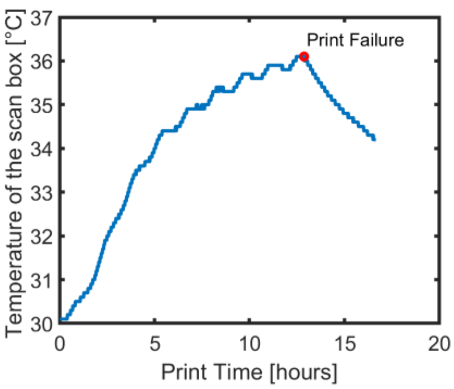

Figure 3. Increase in scan box temperature with print time, as measured by a k type thermocouple positioned on the outer surface of the scan box.

4.1 Measurement Sensitivity

The standard error of measurement in the ring offset was calculated solely from measurements taken on pillar number six. These measurements were repeated 11 times. The maximum standard error across all 8 pucks was 2.4 µm. Fig. 4 shows the plotted averaged values and on top of the box plot generated from the 11 measurements. The variation in ring offset is an order of magnitude greater than the standard error of measurement, therefore a misalignment between the two lasers is clearly occurring. However, there appears to be no discernible trend, as if it was due to thermal expansion, one would expect the offset to be strictly increasing or decreasing.

Since there is not a discernible trend along the height of one pillar, it is difficult to ascribe the variation to the thermal expansion of the laser's elements as this would cause a continuous change.

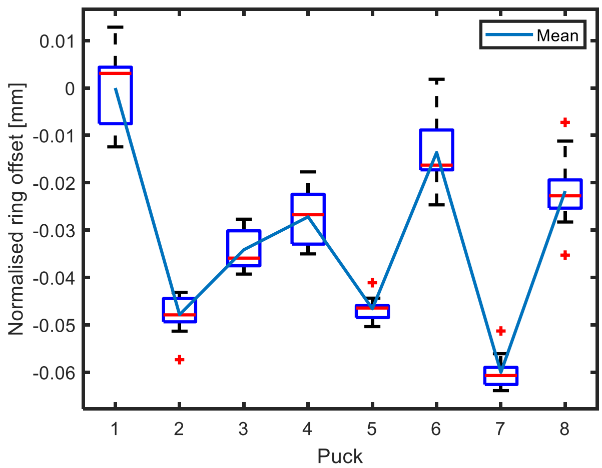

Figure 4. Box and whisker chart of the measurement deviation across 11 separate measurements taken on one pillar.

The measurements of the x and y offsets of the 5 pucks initially analysed show an increase of the x offset and decrease of the y offset, as displayed in Fig. 5. Taking the average across the 5 pillars on the baseplate, the x and y position on the final alignment mark layer are 32 µm and -60 µm respectively.

Equivalent to a total average offset of 68 µm between the two lasers.

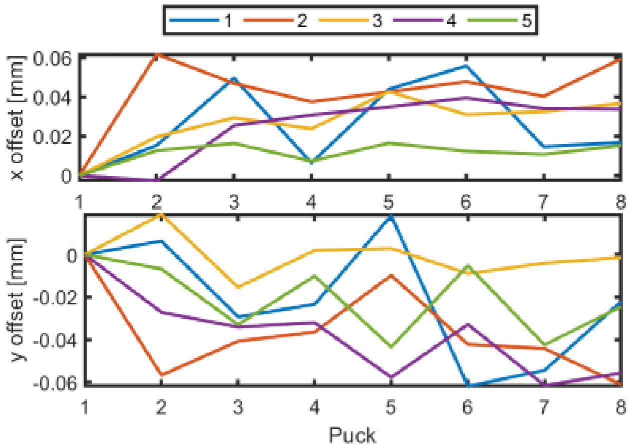

Figure 5. Variation in ring offset for pucks of increasing height taken from 5 different pillars on the baseplate.

Plotting these values on a quiver plot representing the baseplate, with the position of the pillars as displacement centre, reveals a definite trend in the angle at which the displacements occur, with a predominance to the bottom right Fig 6. Inspection of the position of the scan heads is needed, to correlate this to expansion of the scan box.

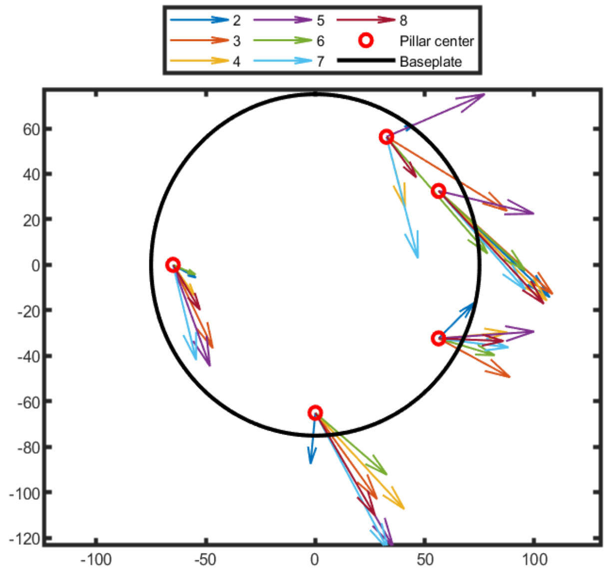

Figure 6. Quiver Plot showing the observed ring offset from at each puck height. Starting from the top, pillars are numbered clockwise one through five. Quivers are automatically scaled for visibility.

5. Discussion and future work

No clear conclusions can be drawn as to the source of the change in offset, however a noticeable change in alignment marks offset was revealed. Since the hatch distance is usually about 100 µm in the LPBF process, the 68 µm average shift detected towards the end of the build has the potential to create sufficient separation in hatches for lack of fusion to occur.

To further investigate this issue, the analysis of all the pillars on the base plate will be completed. This will provide a better understanding of the distribution of the error across the base plate. Furthermore, during the next maintenance of the scan box, measurements will be taken of the relative position of the two scan head. These measurements will be correlated with the observed offset direction from Fig 6. to investigate the possibility of thermal accumulation causing stretching of the scan box.

In future prints, a redesign of the pillar will be considered, replacing the cylindrical pucks with square rectangular prisms. This change aims to facilitate the alignment process in the microscope. Moreover, to enhance the contrast between the alignment marks and the underlying hatches, alignments marks will be printed over two or more layers,

6. Conclusions

In conclusion, the use of support structures to stack alignment marks in the printer provided an effective method for analysing the variation in laser offset during printing. Optical microscopy and curve fitting techniques achieved a standard error of measurement of 2.4 µm for the relative position of the alignment rings. A noticeable offset change of 68 µm was observed after 40 mm of printing, which could adversely affect neighbouring hatches scanned with different lasers. While a predominant direction for this offset was observed, no clear trend in its rate of increase was detected. Further investigation is planned to explore the variation of this increase across the base plate.

References

[1] Goossens, L. R., Kinds, Y., Kruth, J.-P., & Van Hooreweder, B. (2018). "On the Influence of Thermal Lensing During Selective Laser Melting." In Solid Freeform Fabrication Symposium Proceedings (SFF Symp 2018), 2267–2274. Austin; University of Texas.

[2] Schindelin, J., Arganda-Carreras, I., Frise, E., Kaynig, V., Longair, M., Pietzsch, T., … Cardona, A. (2012). "Fiji: An Open-Source Platform for Biological-Image Analysis." Nature Methods, 9(7), 676–682. doi:10.1038/nmeth.2019

[3] Virtanen, P., et al. (2020). "SciPy 1.0: Fundamental Algorithms for Scientific Computing in Python." Nature Methods, 17(3), 261-272.

[4] Hammel, B., & Sullivan-Molina, N. (2020). "bdhammel/least-squares-ellipse-fitting: v2.0.0." Zenodo.